Alexandria Engineering Journal (2022) 61, 1852–1863

HOSTED BY

Alexandria University

Alexandria Engineering Journal

www.elsevier.com/locate/aej
www.sciencedirect.com

Artificial intelligence image recognition based on 5G deep learning edge algorithm of Digestive endoscopy on medical construction

Lili Yang [a], Zhichao Li [b,*], Shilan Ma [c], Xinghua Yang [a]

[a] Endoscopy Center, Linyi Central Hospital, Linyi, Shandong 276400, China
[b] Delivery Room, Linyi Central Hospital, Linyi, Shandong 276400, China
[c] Nephrology Department, Linyi Central Hospital, Linyi, Shandong 276400, China

Received 22 April 2021; revised 17 May 2021; accepted 10 July 2021
Available online 08 August 2021

KEYWORDS

Smart medical construction;
Artificial intelligence image recognition;
5G deep learning edge algorithm;
Digestive endoscopy

Abstract In this paper, we use artificial intelligence image recognition to obtain Digestive endoscopy image, and process the image based on 5G Deep learning edge algorithm to judge the disease type of the patient, and then consider the treatment plan. The combination of body area network and edge computing technology can meet the demand of low delay in body area network. In this case, the resource constrained body area network gateway node can process the physiological data collected by it into an offloadable task, and then unload the task and data to the edge computing node according to a certain strategy. The edge computing node completes the corresponding task processing and data storage, and finally provides the results to the relevant medical institutions and body area network users for reading auxiliary diagnosis and treatment of diseases. Studies have shown that 25% of patients with colon polyps have CD4 cells in peripheral blood based on 5G deep learning edge algorithm under artificial intelligence image recognition of Digestive endoscopy. The number of lymphocyte in group of differentiation was less than 200/μL, and the blood RNA in 92.3% patients was lower than 100 IU/ml, while fam CTP (A-cyclic peptide) was lower than 100 IU/ml. Opportunistic infections of the intestine and viruses can directly cause enteropathy because the fluorescence intensity of the probe is essentially unchanged and cannot form a triple helix structure. In terms of feature recognition accuracy, the 5G deep learning edge algorithm in this paper improves accuracy by 68% compared to the simple Yolo algorithm, and is similar in speed. Compared with RCNN algorithm, the accuracy and speed are improved by 21% and 85% respectively. Therefore, the 5G deep learning edge algorithm based on artificial intelligence image recognition has the advantages of accuracy and speed in digestive endoscopy of intelligent medical.

* Corresponding author.
E-mail address: L15163991062@163.com (Z. Li).

Peer review under responsibility of Faculty of Engineering, Alexandria University.

https://doi.org/10.1016/j.aej.2021.07.007
1110-0168 © 2021 THE AUTHORS. Published by Elsevier BV on behalf of Faculty of Engineering, Alexandria University.

1. Introduction

Smart medicine is a hot topic in recent years, which is a new interdisciplinary subject integrating life science and information science. There is no very clear definition of smart medicine. The mainstream view is that it is based on medical informatization. The core is to manage patient identities through the Internet of Things and sensor technology and form patient indexes in hospital information systems. Based on this, information exchange and communication are performed according to business logic and network protocols to enable intelligent identification and identification location, tracking, monitoring and management.

At present, artificial intelligence image recognition has been applied in the fields of disease imaging and drug treatment. The strategy of image target recognition has been widely studied. For example, Buch V proposed that it is one of the most common methods to observe the cyclization of target peptides through smart medical human body tomography, but the system is unstable in the redox environment, and the synthesis steps are complex [1]. Therefore, the detection of collagen must be heated before pretreatment, which will lead to the risk of tissue damage. Bin Yu thinks that the current smart medicine should be called intelligent medicine or intelligent medicine [2]. F chiariotti made an innovative interpretation and analysis on the intelligent medical treatment of intestinal diseases, in order to open a new door for the effective prevention and control of intestinal diseases [3]. Robert o believes that only with the full participation of traditional Chinese medicine and the final formation of an effective combination of traditional Chinese medicine and Western medicine in theory and clinical practice can we expect to realize the intelligent medical treatment of hypertension [4]. Robert o proposed that no matter how developed the network information is and how high the degree of informatization is, it cannot replace the face-to-face ''seeing, hearing, asking, seeing, touching, listening'' and emotional communication between people [5].

With the development of Internet of things technology, the underlying technology of wireless sensor network has been developed rapidly. As a special type of wireless sensor network in the field of biology and intelligent medicine, wireless body area network has been widely concerned by all sectors of society, including academia, industry and government departments. Inamoto y suggested that the target of blood glucose control during TPN should be 7.8–10 $mmoll^{-1}$. However, considering the abnormal glucose tolerance of the patient, hyperglycemia may also occur. In order to avoid the occurrence of hyperglycemia, insulin 2 UH-1 was pumped alone to control blood glucose [6]. The above studies focus on the disease, and analyze the nature of the disease and the types of protein variation, but compared with the artificial intelligence image recognition technology, there are many shortcomings, and the disease recognition rate of the above studies is low. Body area network is generally composed of sensors deployed in the body, on the body surface or near the body surface. These sensors can obtain the body temperature, blood pressure, blood oxygen, EEG, ECG and other physiological parameters. The physiological parameters collected by each sensor are sent to the body area network gateway device hub (typical device such as mobile phone) through wireless communication, and then sent to the emergency center or doctor through cellular network or Internet for further diagnosis and treatment. After all, people-oriented, rather than disease-based, is the foundation and guarantee for the realization of smart medicine.

In this paper, we use artificial intelligence image recognition to obtain the patient image, and process the image based on 5G deep learning edge algorithm to judge the disease type of the patient, and then consider the treatment plan. Firstly, OPA cyclization method was used to prepare fluorescent artificial intelligence image recognition probe at room temperature. An image of a diseased patient under artificial intelligence image recognition was acquired using a fluorescent artificial intelligence image recognition probe and integrated into the blood vessel recognition result under artificial intelligence image recognition. Then the image decomposition and feature extraction of artificial intelligence image recognition are carried out, and the disease is matched according to the image target recognition results. The original fundus image, u-net network recognition results and CE net network recognition results are compared with the proposed method.

2. Artificial intelligence image recognition and 5G deep learning edge algorithm

2.1. Intelligent medical body tomography

Intelligent medical human body tomography is the preferred method for the diagnosis and treatment of colorectal diseases. Ordinary intelligent medical human body tomography injects air. Because the air injected into the intestinal tract is not easy to be absorbed, it is easy to lead to intestinal extension, intestinal cavity expansion, and even intestinal angular loop, resulting in abdominal pain and abdominal distension, and even the risk of inducing perforation and air embolism [7]. This may be related to the fact that it takes more time for water exchange colonoscopy to distinguish the shape of the intestinal cavity by water injection through the lumen when entering the colonoscopy, to suck out the residual air and feces in the intestinal cavity to clean the intestinal tract, and to pump out the excess water in the intestinal cavity when withdrawing the colonoscopy, and to improve the detection rate of lesions until the observation time is prolonged. The research results are consistent with the meta analysis results of water injection method and air injection method of human body tomography in smart medicine [8]. Based on the peptide sequence (Gly Pro Hyp) n and OPA cyclization method, this new collagen targeted artificial intelligence image recognition probe fam CTP can maintain the single chain state, and can specifically identify the pathological collagen in different types of connective tissue, which has a good application prospect in the detection of collagen [9–10]. For the non preheated fam CTP, only the denatured collagen coated well plate showed strong fluorescence in all 96 well plates examined by smart medical human tomography, indicating that fam CTP can specifically bind denatured collagen without heating [11–12]. At the same time, all 96 well plates stained by fam in blank control showed very low fluorescence intensity, because fam could not bind any target protein. Compared with denatured collagen, the binding ability of fam CTP to normal collagen and other proteins is extremely low, indicating that the artificial intelligence image recognition probe fam CTP has strong targeting specificity for denatured collagen [13–14]. Smart medical human body tomography tar-

geted fluorescence imaging can observe the targeted binding ability of fam CTP, fam-ctp and classic collagen targeted fam-gpo probes to pathological collagen through tissue staining [15–16]. Fam CTP keeps single strand state, and can recognize pathological collagen without any pretreatment. At the same time, the imaging results of damaged cartilage tissue showed that fam CTP had a strong ability to bind the pathological collagen, and the introduction of C-terminal ring structure did not affect the ability of polypeptide probe to recognize the pathological collagen. Collagen-targeted fluorescent artificial intelligence image recognition probe (Gly Pro Hyp) n-sequence design can target and bind affected collagen, but forms a triple helix structure and is capable of targeting and binding. Based on the (Gly Pro Hyp) n sequence, the fluorescent artificial intelligence image recognition probe famCTP was constructed by cyclization modification. The ring structure can inhibit the probe to form triple helix structure, thus maintaining the single chain state, and will not affect the ability of the probe to recognize collagen [17–18].

2.2. 5G deep learning edge algorithm based on artificial intelligence image recognition

The monogenic signal can be used for multi-target recognition, decomposition and feature extraction in artificial intelligence image recognition image

$$R = \arctan2\left(z, \pm\sqrt{x^2+y^2-z^2}\right) - \arctan2(I,J) + T \tag{1}$$

where R is the Riesz transform of the input image, I and j are imaginary units. According to the above formula, three kinds of single signal characteristics are defined

$$^{y}k = y + 1yA\,y + 2y + 1A \ldots z - 2z - 1A\,zz - 1A\,^{z}k \tag{2}$$

where a and K are the components of the single signal on the two axes respectively; y and Z reflect the phase component and azimuth information respectively. The three kinds of single signal features can effectively reflect the multi-level characteristics of the image, including local amplitude, phase and direction characteristics. By combining these three types of features, more sufficient information can be provided for image analysis [19–20]. For this reason, this paper uses the single signal to describe the image features of each sub block. According to the ideas of literature, the three types of features are vectorized, concatenated and downsampled to obtain the low dimensional feature vector. Finally, each sub block is classified based on the feature of single signal. Classification sparse representation classifies the unknown samples according to different categories, and makes a decision by the size of the fitting error. At present, sparse representation classification has been widely used and verified in AI image recognition. For the test sample y, the sparse representation process is as follows:

$$^{0}C = 10A\,21A - - - x - 1x - 2A\,xx - 1Ak \tag{3}$$

where a represents the global dictionary composed of C training categories, which is sparse in 08 norm and mathematics. SRC is used to analyze and process the four sub blocks of the original AI image recognition image, and their corresponding reconstruction error vectors are obtained [21–22]. The results of different sub blocks are fused by linear weighting. But considering the limitation of a single fixed weight vector, this paper uses multiple groups of random weight vectors to process, and the weight matrix is designed as follows

$$y_{it} = \alpha_0 + \alpha_1 Dmax_{it} + \alpha_2 X_{it} + \mu_i + \eta_t + \alpha_{it} \tag{4}$$

$$U_2 = \begin{cases} s - p_1 - kx_2 \\ x - p_2 - k(1-x_2) \end{cases} \tag{5}$$

In the formula, each column corresponds to a group of random weight vectors, which satisfies the following constraints:

$$\Delta_{ikjl}(\varepsilon) = \begin{cases} 0, x_{ik}(\varepsilon) = N/A \; or \; x_{jl}(\varepsilon) = N/A; \\ 1, x_{ik}(\varepsilon) = N/A \; and \; x_{jl}(\varepsilon) = N/A \end{cases} \tag{6}$$

$$x_1 = \frac{p_2 - p_1 + k}{2k} \tag{7}$$

Under the constraint of equation (6), each group of weight vectors is determined randomly, and N groups of random weight vectors are obtained. Each group of weight vector may give different weights to different sub blocks, and the final result can obtain the fusion result more effectively, which effectively avoids the instability caused by traditional weight determination. Note that the reconstruction error of class I for the k th sub block is C, and the random weighted fusion is described as:

$$p_1^* = \frac{2k}{k+1} + \frac{2c_1 + c_2 + 3et + 2et\zeta}{3} \tag{8}$$

$$I = \frac{n\sum_{i=1}^{n}\sum_{j=1}^{n}\left(x_i - \bar{x}\right)\left(xj - \bar{x}\right)}{\sum_{i=1}^{n}\sum_{j=1}^{n} w_{ij}\left(xi - \bar{x}\right)^2} = \frac{n\sum_{i=1}^{n}\sum_{i\neq j}^{n} w_{ij}\left(x_i - \bar{x}\right)\left(xj - \bar{x}\right)}{S^2\sum_{i=1}^{n}\sum_{j=1}^{n} w_{ij}} \tag{9}$$

On the basis of equation (8), the ownership value vector in equation (9) is used to repeat the operation, and the class I has n results, which are recorded as the fusion error vector [23–24]. If class I is the actual class, the reconstruction errors of each sub block are small. At this time, in the random weight vector, the values of each element in the fusion error vector are small and change gently. On the contrary, if the current test sample is not from class I, the reconstruction error of each sub block is relatively large

$$P\left(d_i, w_j\right) = P(d_i)P\left(w_j|d_i\right); P\left(w_j|d_i\right) = \sum_{k=1}^{K} P\left(w_j|z_k\right)P(z_k|d_i) \tag{10}$$

$$\frac{\partial \pi_B^{LH}}{\partial p_2} = \frac{1 - p_2 + p_1}{2} - \frac{p_2 - c_2}{2} + \frac{k - p_2 + p_1}{2k} - \frac{p_2 - c_2}{2k} - et\left[-\frac{1}{2} - \frac{1}{2k}\right] = 0 \tag{11}$$

According to equation (11), the decision variables corresponding to each category can be calculated respectively, and the category with the minimum value is judged as the real target category of the test sample. The image segmentation algorithm is used to process all training samples, and the feature vector of each sub block is extracted. On this basis, the dictionary of each sub block is formed [25]. For the test sample, the corresponding block operation is carried out and the cor-

responding single feature vector is obtained. Finally, according to the decision variables of different categories, the target category is obtained

$$SRC(k) = [\zeta_1 c_1(t) + \zeta_2 c_2(k) + \zeta_3 c_3(k) + \zeta_4 c_4(k) + \zeta_5 c_5(k) + \zeta_6 w_{ik}] \tag{12}$$

$$c_1(t) \geqslant 0, c_2(k) \geqslant 0, c_3(k) \geqslant 0, c_4(k) \geqslant 0, c_5(k) \geqslant 0 \tag{13}$$

$$\zeta_1 + \zeta_2 + \zeta_3 + \zeta_4 + \zeta_5 + \zeta_6 = 1 \tag{14}$$

Based on the correlation understanding of compressed sensing, sparse representation uses dictionary representation to describe and analyze the new samples, and then analyzes the characteristics of the samples according to the reconstruction results. Assume that the global dictionary is:

$$\min w_k(t) = \left[\omega_1\left(\frac{d_k}{V}\right) + \omega_2\left(\frac{d_k}{V}\right) + \omega_3\left(\frac{T_k}{ND_K}\right) + \omega_1(P_K T_K)\right] \tag{15}$$

where W is the coefficient vector with sparsity (that is, there are only a few non-zero elements); it represents the final reconstruction error. The minimum reconstruction error criterion, which is widely used in the existing literature, investigates the representation ability of different training classes for test samples through the reverse idea of sparse representation, and has strong reliability. In addition, if the test samples come from the extended operation conditions and are different from the training samples, the fault tolerance rate of relying solely on the global minimum reconstruction error is low. Therefore, in this paper, we will design two other criteria to supplement them. In sparse representation frameworks, non-zero coefficients are usually distributed to the actual corresponding categories of test samples. Therefore, the coefficient energy of the correct category is relatively high. Under maximum coefficient energy criteria, test samples must maintain a high correlation with some samples in a particular training category in order to obtain large coefficient energies. The overall energy of the coefficient will not be very high. This is often difficult to reflect in the minimum reconstruction error criterion. The reconstruction of each category should be considered in the local dictionary.

3. Intelligent medical multi-target recognition

3.1. Methods

In this paper, we use artificial intelligence image recognition to obtain the patient image, and process the image based on 5G deep learning edge algorithm to judge the disease type of the patient, and then consider the treatment plan. The combination of body area network and edge computing technology can meet the demand of low delay in body area network. In this case, the resource constrained body area network gateway node can process the physiological data collected by it into an offloadable task, and then unload the task and data to the edge computing node according to a certain strategy. The edge computing node completes the corresponding task processing and data storage, and finally provides the results to the relevant medical institutions and body area network users for reading auxiliary diagnosis and treatment of diseases.

3.2. Design

This paper proposes a body area network intelligent medical system architecture assisted by edge computing, and uses this architecture to study the pathology of 64 patients in the First Affiliated Hospital of Nanchang University. The edge computing technology is used to realize the real-time processing of human physiological parameters in body area network, and the corresponding task unloading algorithm is designed and simulated. The simulation results are consistent with the theoretical analysis results. Time delay, received signal strength and load are taken as the evaluation criteria of the target node. The algorithm can adjust the relevant evaluation criteria adaptively according to the urgency of the task. According to the different characteristics of tasks from the gateway node of body area network, the target edge computing node adopts different task processing strategies. If the task is urgent, it will be preemptively scheduled; otherwise, it needs to be queued according to the scheduling strategy of first come first served (FCFS), and it can only be processed after the task in the queue of the target edge computing node is processed.

After training mask r-cnn and yolov3 disease detection models, DAPI was used to stain the nucleus to show blue, so as to co localize collagen. The results of tissue staining showed that fam CTP could specifically bind to denatured collagen in various types of tissues without pre heating. Artificial intelligence image recognition probe targeted fluorescence imaging of human pathological tissue using artificial intelligence image recognition probe fam CTP to further stain liver fibrosis, liver cancer, lung cancer and rectal cancer tissue. Fluorescence micrographs showed strong green fluorescence, indicating that fam CTP can specifically recognize denatured collagen in various pathological tissues. The results of protein binding and tissue staining showed that famCTP can specifically bind to denatured collagen without preheating the protein. When the three probes were not pre heated, only fam CTP could stain the pathological collagen in the damaged cartilage tissue, while after pre heating, all the three polypeptide probes could bind to the pathological collagen. These results once again showed that only the single chain polypeptide probe could bind to the pathological collagen, while the triple helix polypeptide probe completely lost its ability to bind to the pathological collagen.

4. Results and discussion

4.1. Artificial intelligence image recognition on intelligent medicine

The results of blood vessel recognition under artificial intelligence image recognition are shown in Fig. 1. In the above figure are the original fundus image, u-net network recognition results and CE net From the network recognition results and the recognition results of this method, we can see that the recognition effect of this method is better for the subtle and complex blood vessels, including the bifurcation or endpoint of the subtle blood vessels. Compared with the previous methods, this method has a good improvement effect, and can better assist doctors to carry out diagnosis and further observation.

The quantitative evaluation index results are shown in Table 1. This paper compares the recognition effects of the

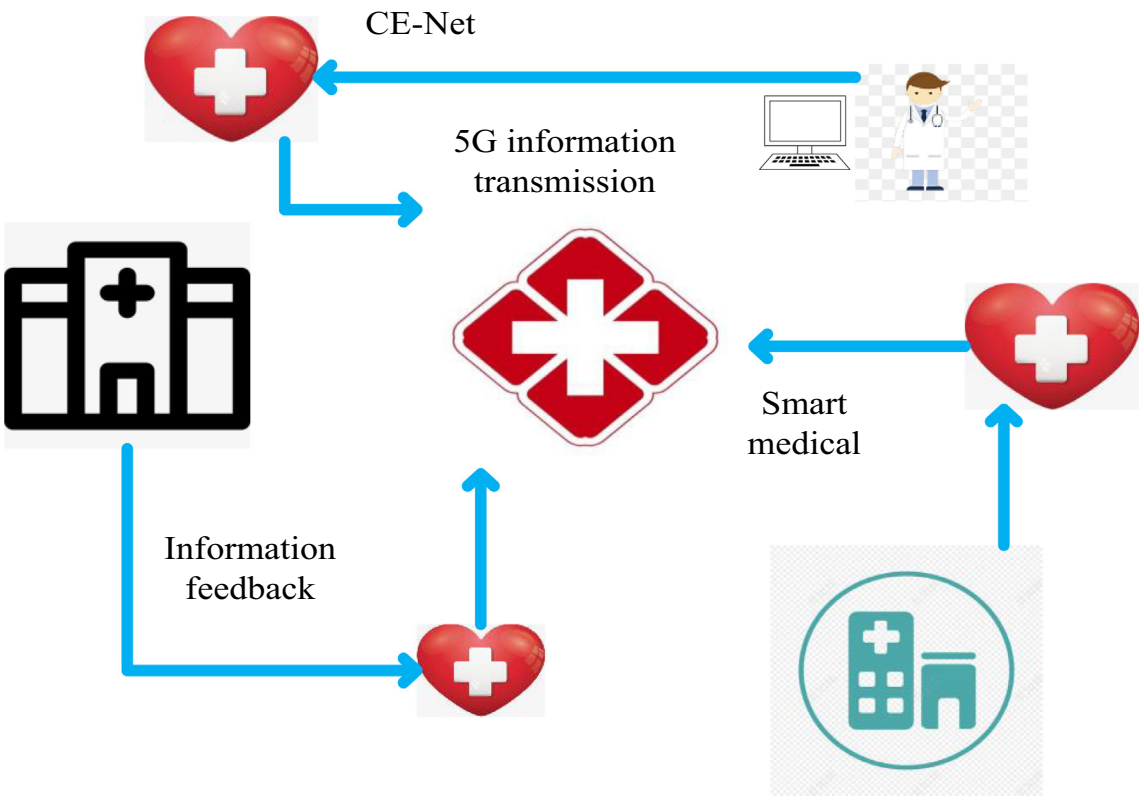

Fig. 1 Digestive tract vessel segmentation results (Some pictures are from CNKI).

Table 1 Quantitative evaluation index results.

Item	Exudate	Bleeding point	U-Net	CE-Net	Ground	Adenoma
Inflammatory	0	0.21	1.98	0.2	0.13	0.63
Backbone	3.43	2.97	1.02	3.08	3.67	3.15
New RMP	4.37	2.13	5.4	2.98	5.41	4.87
New DAC	2.72	2.24	5.69	3.86	2.56	1.04
HAM	4.67	1.18	4.26	3.58	3.66	4.06
MSTAR	4.07	2.86	1.03	5.28	1.76	6.37

dense hole convolution module and the residual multi-scale pooling module in the context extraction coding module based on the backbone network. It is found that the improved residual multi-scale module can improve the recognition effect better. It can effectively facilitate network recognition of high-level contextual features for features of retinal vessels and bleeding spots that are distributed throughout the image. Use of information to improve the effectiveness of network awareness. Based on the backbone network, this treatise improves the context extraction coding module, further improving its effectiveness. It can be seen that a more comprehensive integration and utilization of high-level features has a good role in promoting the network effect, and can improve the overall recognition effect, but the AUC value is not significantly improved, so the ability of subtle blood vessel recognition is generally improved.

As shown in Table 2, each decision criterion can make an independent decision according to the coefficient vector solved. If the decision-making of each criterion is consistent, they confirm each other, so the reliability of decision-making is very high. However, if the results of the three criteria are inconsistent, it is necessary to integrate their results scientifically to obtain more reliable results. Firstly, the reconstruction error and coefficient energy are transformed into a unified form.

In order to promote the application of the Internet of Things in smart cities, this article proposes a strategic roadmap for the Internet of Things, which is expected to provide a large amount of funds by 2022. In this regard, by using sensors integrated into the Internet through a wireless communication system, data can be collected from inanimate and living things. In addition, the plan of the smart medical project is based on the ambition of transforming a metropolis into a smart city based on IoT technology. As shown in Fig. 2, by using IoT technology, many industries will be transformed into smart services, especially energy, transportation, and healthcare industries.

As shown in Fig. 3, the performance of each method is affected by the model difference. For cnn1 and cnn2 methods

Table 2 Experimental segmentation results of bleeding points of exudate.

Item	Exudate	Bleeding point	U-Net	CE-Net	Ground	OCR
Adenoma	2.99	1.65	3.55	3.79	2.55	1.3
Inflammatory	5.14	5.9	5.91	5.41	5.33	3.82
Backbone	4.06	4.52	3.74	2.7	4.77	4.37
New RMP	2.39	4.54	2.55	3.03	3.77	1.81
New DAC	1.62	1.98	5.63	6.82	6.83	6.49
HAM	3.11	1.99	1.81	2.64	3.52	3.17

based on deep wash, the final average recognition rate decreases most significantly due to the difference of models. In this paper, the test OCR image is divided into blocks, and the local analysis is carried out. Therefore, it is useful to thoroughly investigate the local image changes caused by different models. However, at 45°, the difference in pitch angle has a large effect, and the average recognition rate of each method drops significantly. This shows that different pitch angles make a big difference in OCR images. Similar to the case of model difference, the performance degradation of cnn1 and cnn2 methods is the most significant. Through image block matching, multi weight fusion and statistical analysis, this method can better analyze the local changes of the target, and then obtain reliable decision results through statistical analysis.

As shown in Fig. 4, the fluorescent artificial intelligence image recognition probe was prepared at room temperature. The mass spectrometry results showed that the new artificial intelligence image recognition probe fam labeled with CCTP, control peptide CTP and fam fluorescein - CTP and fluorescent control peptide probe fam - CTP has been synthesized successfully. The ability of fluorescent artificial intelligence image recognition probe to form triple helix structure, triple helix tendency is the key index of collagen targeted peptide probe. Compared with the linear peptide CTP, the circular dichroism (CD) results showed that there was a characteristic peak of triple helix structure at 225 nm. The thermal change experiment showed that the thermal change temperature of CTP triple helix structure was 59 °C.

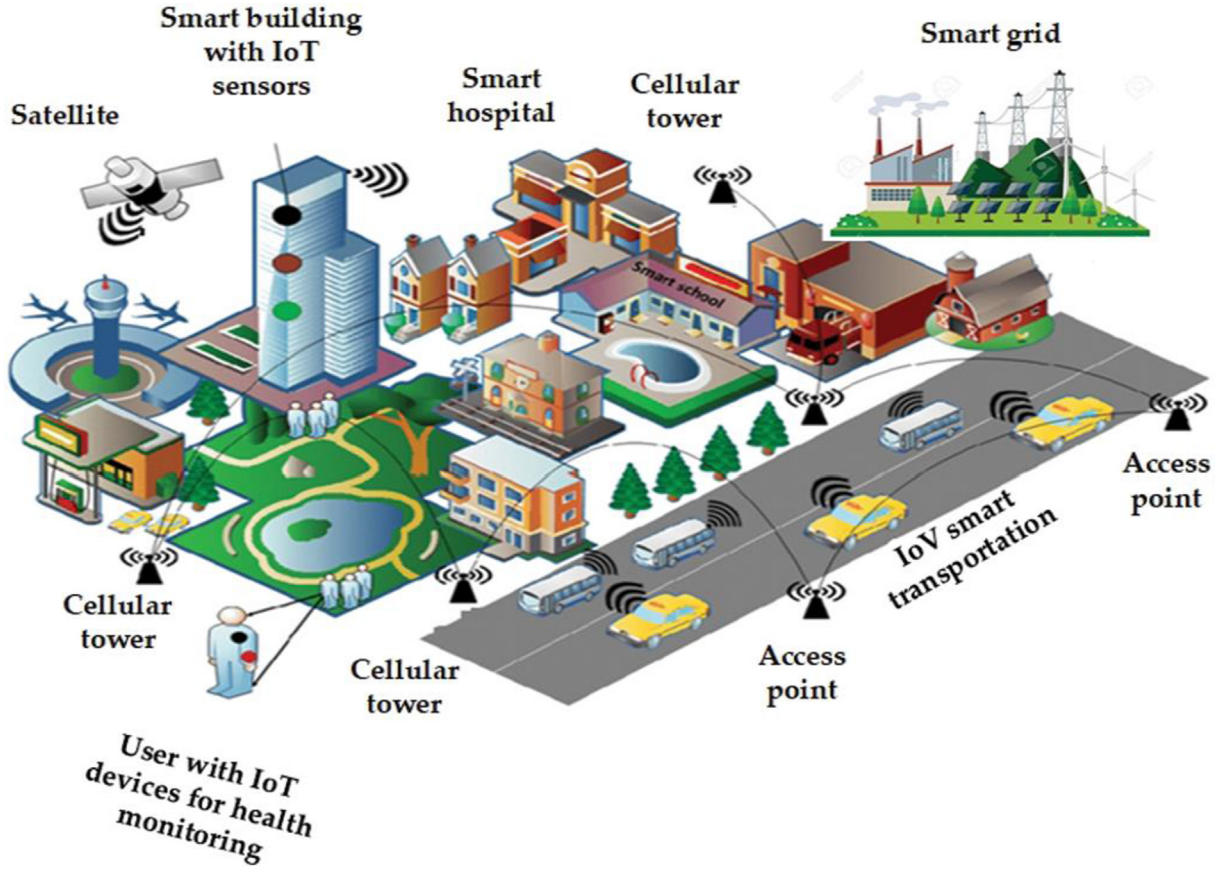

Fig. 2 Schematic diagram of identifying denatured collagen (Some pictures are from Google).

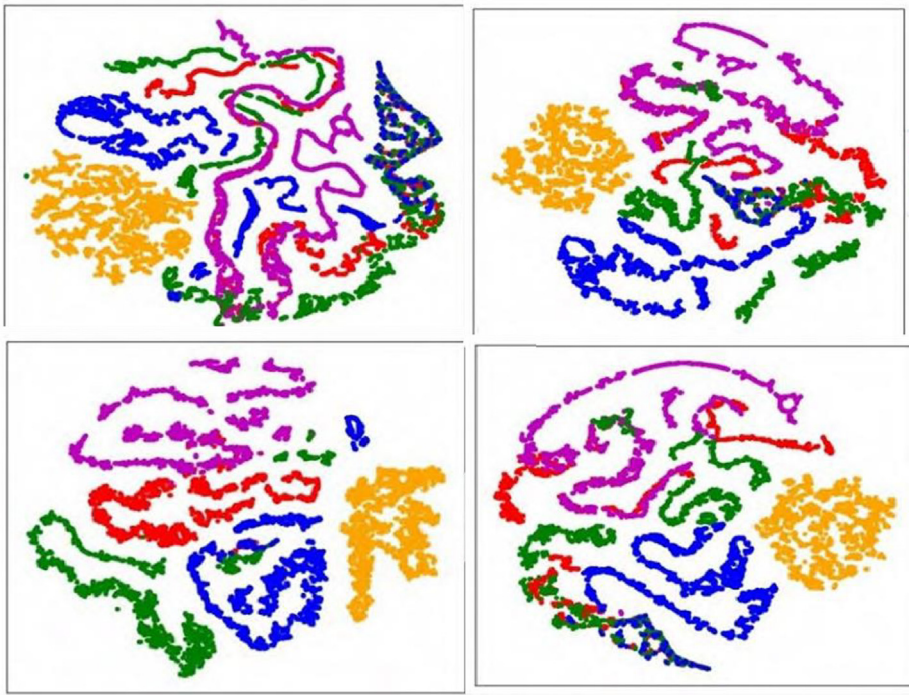

Fig. 3 Each method is subject to model differences (Some pictures are from CNKI).

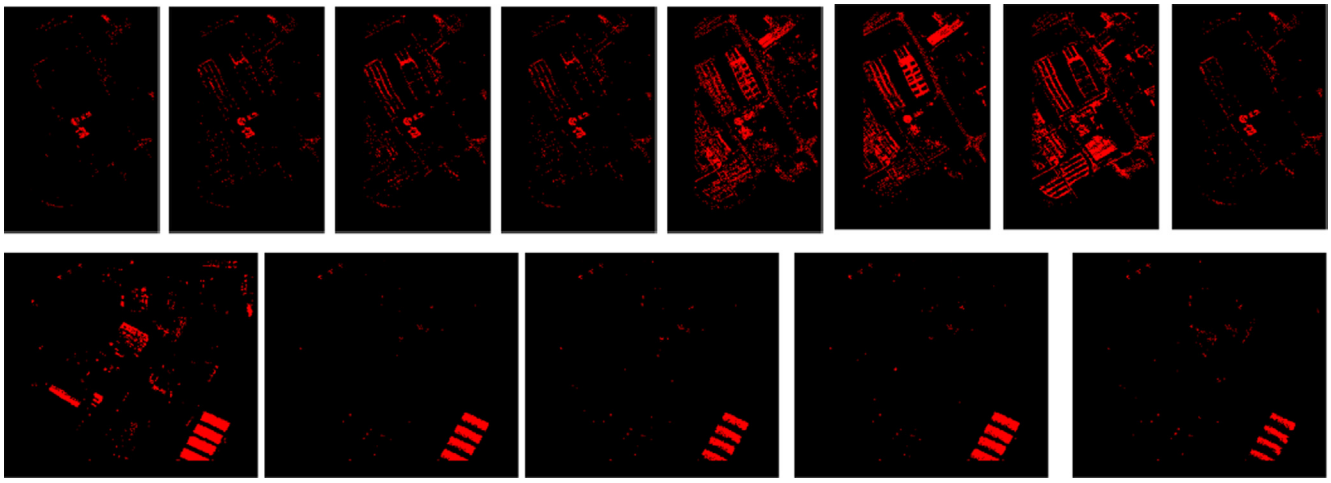

Fig. 4 Fluorescence colonoscopy guide probe (Some pictures are from CNKI).

As shown in Fig. 5, there is no characteristic peak at 225 nm for AI image recognition CTP, and the unfolding process changes linearly, indicating that AI image recognition CTP maintains a single chain conformation and cannot form a triple helix structure. Artificial intelligence image recognition probe fam - CTP and fam - The ability of CTP to form triple helix structure was further studied by fluorescence experiments. FAM - The weak fluorescence of CTP at 4 °C is due to the self quenching of fam due to the close packing of three peptide chains in its triple helix structure; However, the strong fluorescence at 80 °C is due to the recovery of fluorescence due to the monomer state after heating. The overlapping fluorescence spectra of the CTPs before and after heating at 4 °C show that the triple helix structure can be completely refolded by heating and cooling. However, the artificial intelligence image recognition probe fam -CCTP shows the same strong fluorescence at 4 °C, 80 °C, and 4 °C, indicating that it remains single-strand. The refolding ability of the two polypeptide probes was further studied by real-time monitoring the fluorescence intensity at 541 nm.

As shown in Fig. 6, the possible causes of colonic polyps include low intestinal immune function, easy occurrence of various special infections and inflammatory reactions, continuous damage of intestinal mucosa caused by chronic inflammation, resulting in continuous proliferation of cells, long-term direct stimulation of intestinal glands, and then occurrence of meat like hyperplasia. Due to the differences of background, sensors and other factors, the test samples to be

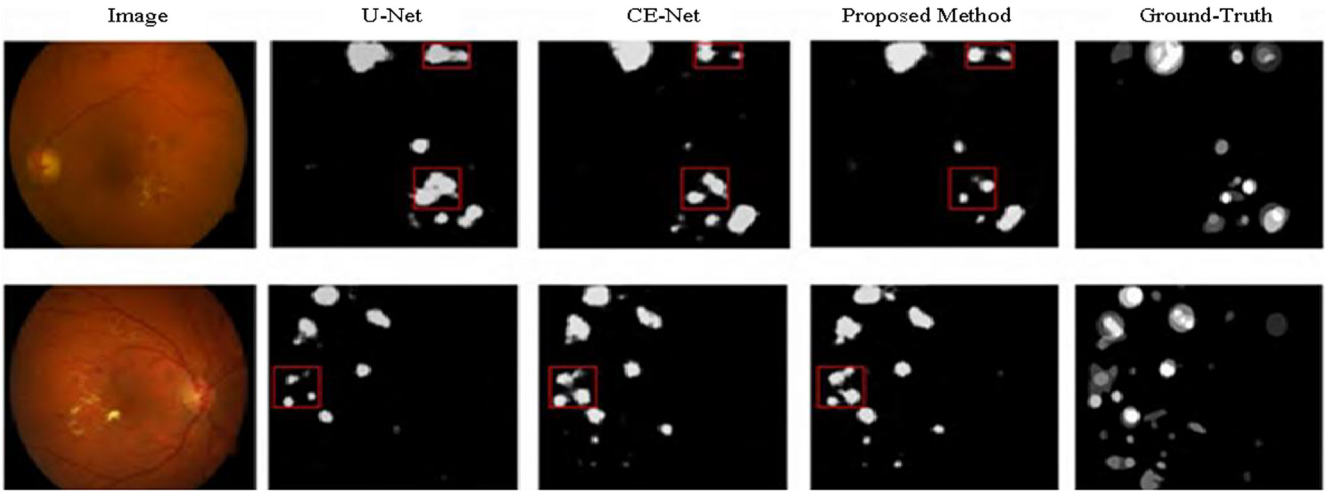

Fig. 5 The unfolding process changes linearly (Some pictures are from CNKI).

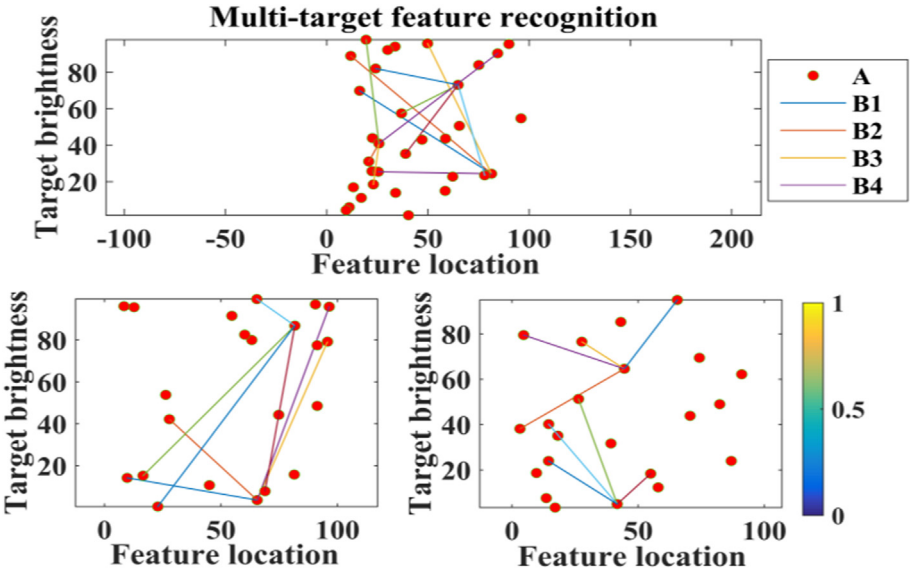

Fig. 6 Multi-target feature recognition.

identified are quite different from the established training samples. Therefore, to solve the difficult problems in the extended operation is the research focus of the current OCR target recognition method. Generally, OCR target recognition methods improve recognition performance by finding the best combination of features and classifiers. In the aspect of feature extraction, the object geometry is described by region and contour, and the object recognition method is designed. The characteristics of gray distribution can be described by means of mathematical transformation or signal processing.

As shown in Table 3, there was no abdominal pain and discomfort, no abdominal physical examination difference, and no perforation sign on abdominal CT. Aspiration pneumonia: patients without cough and expectoration discomfort, lung CT no difference, not considered. Although the cause of high fever is not clear, we should be fully aware of the potential risk of intelligent medical human body tomography for HIV patients. Therefore, when HIV patients underwent painless intelligent medical tomography and polyp extraction, we should fully assess the patient's condition, do endoscopic decontamination in strict accordance with the specifications, reduce the occurrence of routine and special complications, and reduce the pain of patients. This study shows that the main clinical manifestation of HIV patients with colon polyps is diarrhea, but the relationship between the number of CD4+ lymphocytes and HIV RNA and colon polyps needs further study.

The results of different methods are shown in Fig. 7. The proposed method can maintain more stable performance with noise weighting. With the decrease of SNR of test samples, the performance of cnn1 and cnn2 methods based on 5G deep learning decreases significantly. The performance of scattering center matching method is relatively robust under the condition of noise interference. The main reason is that the noise impression is effectively removed in the process of attribute scattering center extraction.

As shown in Fig. 8, the results fully verify the performance advantages of the proposed method under noise interference. When the test sample is in a low SNR, there will be a big dif-

Table 3 Physical signs of patients with digestive tract diseases.

Item	HAM	Exudate	Bleeding	U-Net	CE-Net	New RMP	New DAC
Colonoscope	3.51	2.17	3.43	2.97	1.02	3.08	3.67
Intestinal polyps	3.57	3.14	4.37	2.13	5.4	2.98	5.41
Adenoma	1.52	5.58	2.72	2.24	5.69	3.86	2.56
Inflammatory	4.93	4.5	4.67	1.18	4.26	3.58	3.66
Backbone	5.88	4.51	4.07	2.86	1.03	5.28	1.76

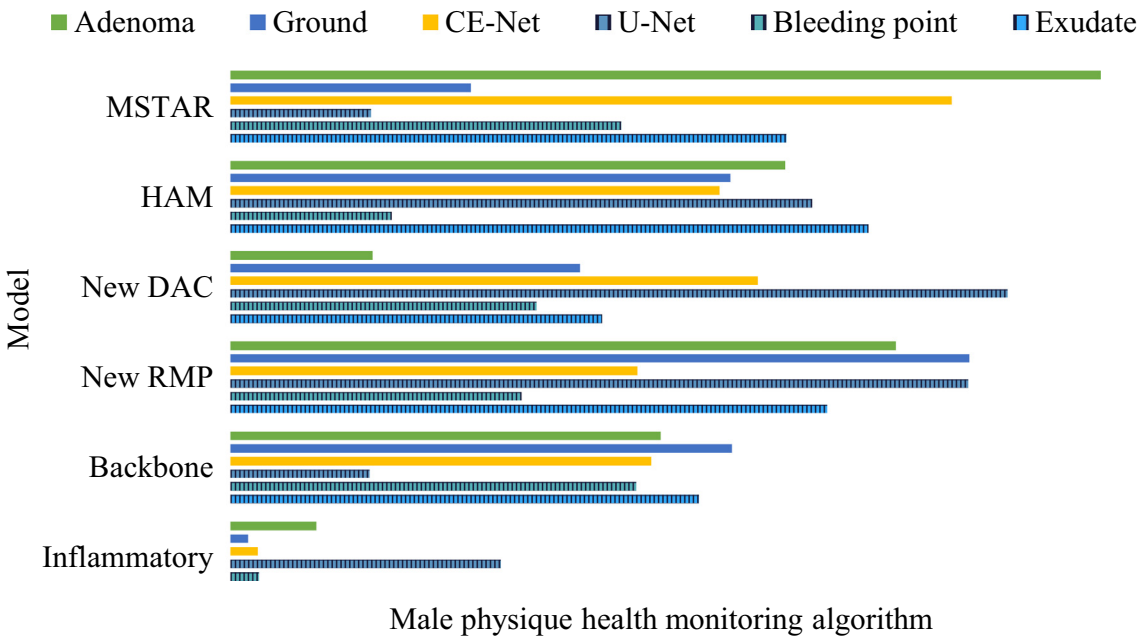

Fig. 7 Signal-to-noise ratio of the test sample.

ference between the test sample and the high SNR test sample, which will lead to the difficulty of recognition significantly increased. The original MSTAR test sample is taken from the same SNR as the training sample. It cannot be used directly to test the noise robustness of the OCR target recognition method. Therefore, in this paper, we first acquire and verify a noise test set due to noise generation. Method noise is reduced. In terms of feature recognition accuracy, the 5G deep learning edge algorithm in this paper improves accuracy by 68% compared to the simple Yolo algorithm, and is similar in speed. Compared with RCNN algorithm, the accuracy and speed are improved by 21% and 85% respectively. Therefore, the 5G deep learning edge algorithm based on artificial intelligence image recognition has the advantages of accuracy and speed in the construction of intelligent medical treatment. In addition, multi-target recognition is conducive to the multi-level diagnosis of diseases.

As shown in Fig. 9, the highest recognition rate of parts under smart medical human body tomography image can reach 94.5%. The incidence of colon cancer is closely related to colon adenoma, and the direct pathogenic role of HIV in the intestine and the risk of opportunistic infection are significantly increased. Therefore, HIV infection rate is high. In this study, the majority of HIV colon polyps occurred in the sigmoid colon, of which 61.5% were tubular adenoma with low-grade intraepithelial neoplasia, which was consistent with the common people's colon polyp prone location and polyp pathology. Through this retrospective analysis, it was found that one HIV patient with colon polyps developed chills and high fever in a short time after painless intelligent medical human body tomography, accompanied by leukopenia and obvious increase of high-sensitivity C-reactive protein.

As shown in Fig. 10, due to the disturbance of protein synthesis and the influence of exogenous amino acid infusion, the laboratory test indexes cannot accurately assess the nutritional status. In addition, due to the influence of peripheral edema, ascites and other factors, there is no evaluation tool suitable for all patients at home and abroad. Subjective global assessment (SGA) has good repeatability, but strong subjectivity. Compared with other objective nutritional indicators, SGA underestimates the incidence of sarcopenia in patients with liver disease. Foreign scholars propose to increase BMI and arm muscle circumference on the basis of SGA, and calculate dietary intake. The evaluation result is objective, but it is time-consuming and inconvenient to operate. The nald index proposed by Chinese scholars still needs to be verified by evidence-based and large-scale clinical practice.

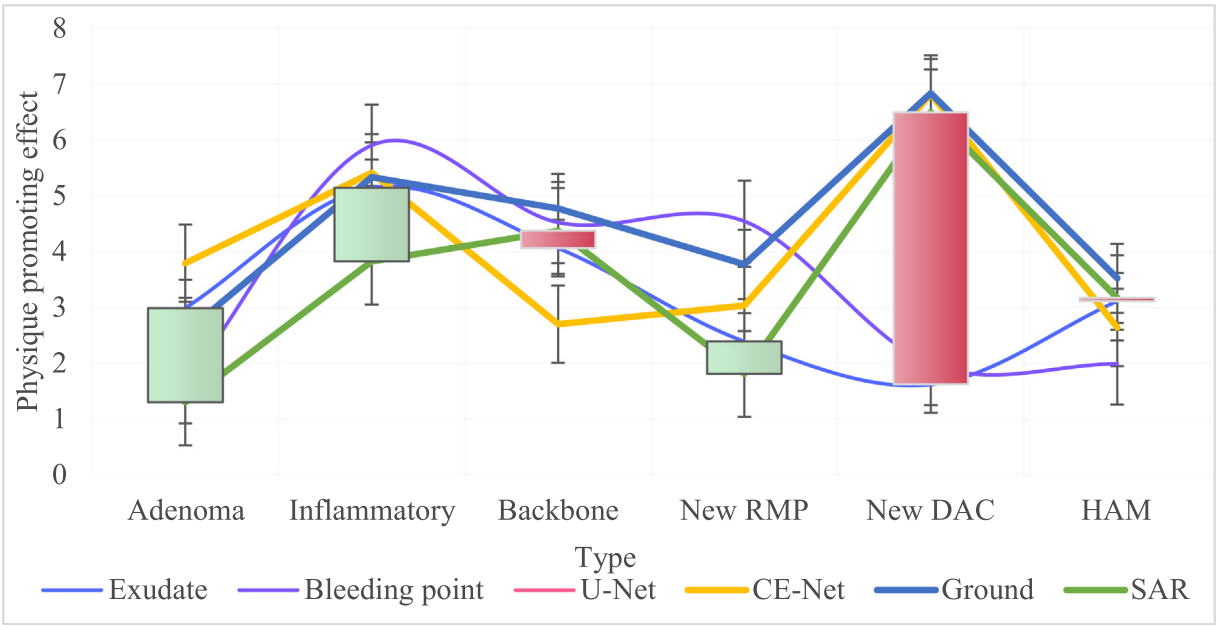

Fig. 8 Performance advantages under noise interference.

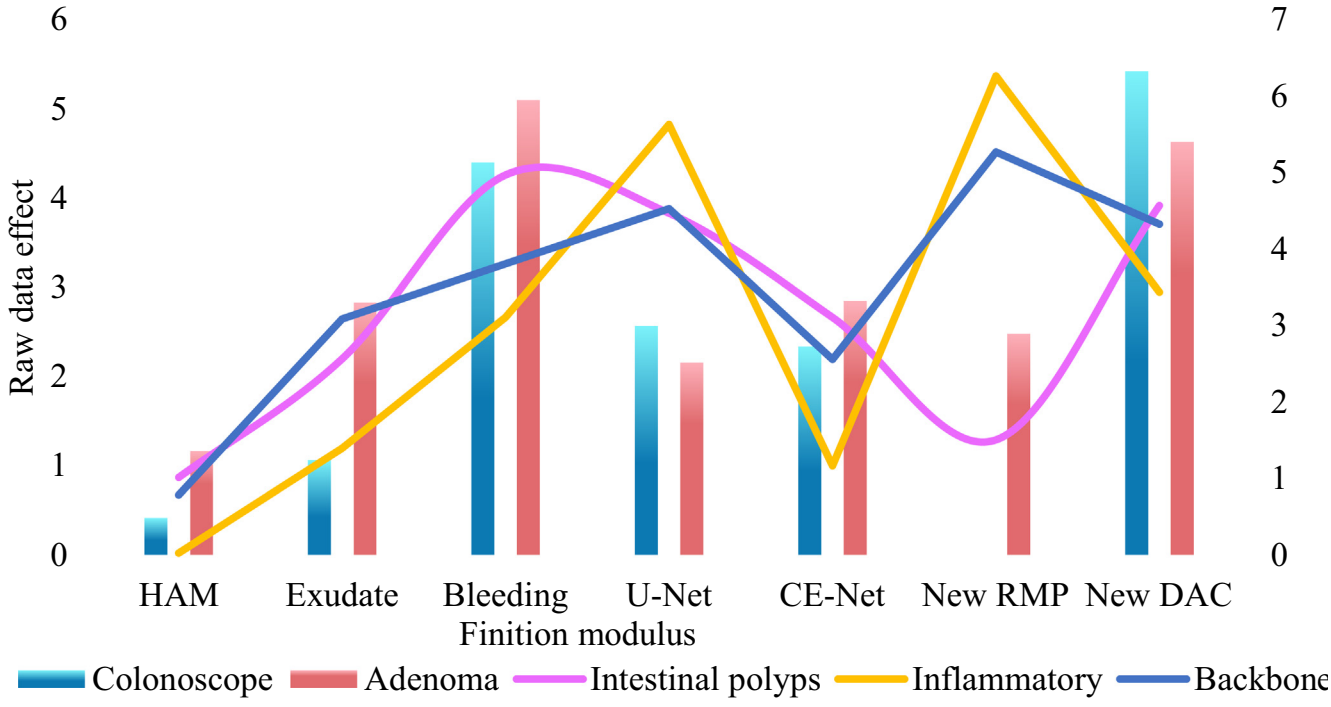

Fig. 9 Recognition rate of parts under colonoscopy images.

4.2. Discussion

Based on the pre training model of mask r-cnn and yolov3, the user-defined model is obtained by fine-tuning, which can recognize the target and recognize it in digestive endoscopy. Among them, yolov3 model is superior to mask r-cnn in speed, but the number of detected targets is more than 30% less than the latter, and the positioning accuracy of targets is at least 10% higher than the latter, which is far behind the literature experiment of yolov3. In the accuracy of digestive endoscopy, the 5G deep learning edge algorithm in this paper improves the accuracy by 68% compared with the simple Yolo algorithm, and the speed is similar. Compared with RCNN algorithm, the accuracy and speed are improved by 21% and 85% respectively. Therefore, the 5G deep learning edge algorithm based on artificial intelligence image recognition has the advantages of accuracy and speed in the digestive endoscopy of intelligent medical treatment. In addition, multi-target recognition is conducive to the multi-level diagnosis of diseases.

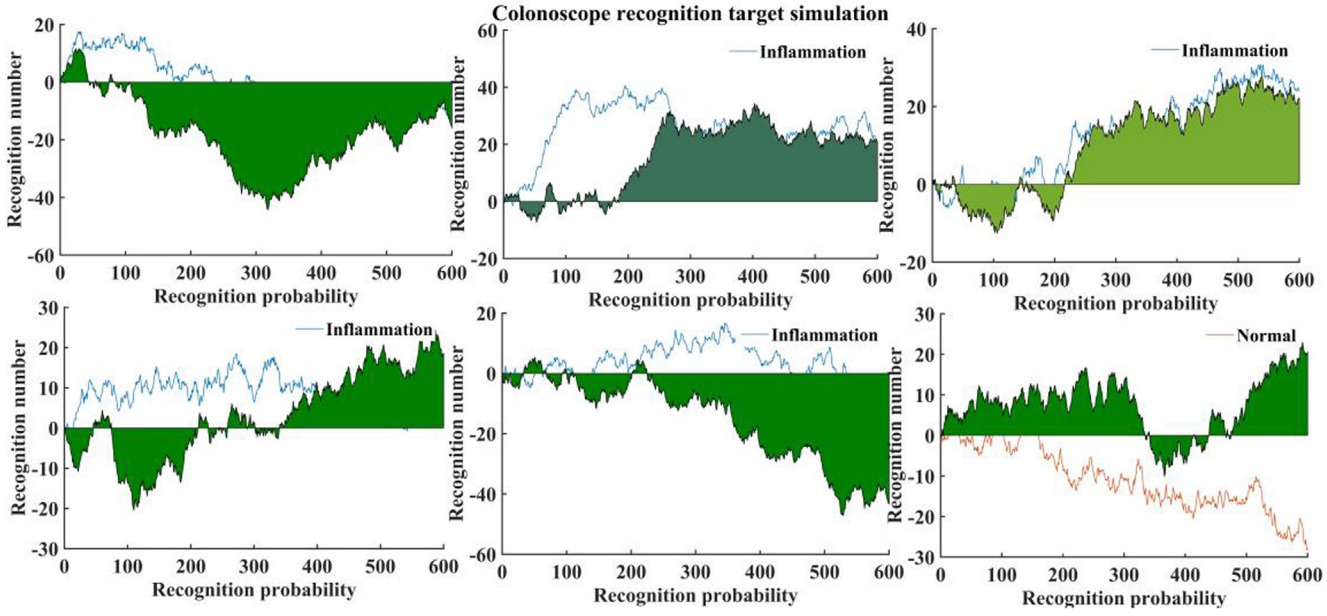

Fig. 10 Colonoscope recognition target simulation.

Since mask R-CNN is the representative of two-stage instance recognition algorithm and yolov3 is the representative of one-stage algorithm, the disease detection model is based on these two algorithms for data set preparation. The digestive endoscopy target detection model is trained, and the frozen model is applied to subsequent detection. 5G deep learning requires that the wider the coverage of the data set (this article refers to disease-related pictures), the stronger the generalization ability of the trained model. The training did not use data enhancement technology, and the images used for training and testing were original images for comparison with subsequent experiments. Because the color, surface texture and even appearance of the disease have great changes in different periods from picking to subsequent sorting and processing, in order to enrich the sample set, some of the experimental pictures are taken from the scene and some from the Internet.

5. Conclusions

According to the medical characteristics of intelligent medical human body tomography, the original OCR image is divided into four blocks, and each sub block reflects the local characteristics of different directions. A single signal is used to describe the spectral and local features of each subblock and build a feature vector. A single feature vector of the four subblocks is categorized by the SRC to get the reconstruction error vector. The four subblock reconstruction error vectors are weighted and fused based on a random weighting matrix. Through statistical analysis of the fusion results of multiple groups of weight vectors, the decision variables are designed and sample categories are obtained. Four test conditions were set in MSTAR dataset, including standard operating conditions and extended operating conditions. Strengthening the construction of medical humanities may help us to arouse our self-contained medical emotions and wisdom, guide us to understand the truth behind medicine, get rid of blind adherence and superstition to medical science and technology, and return to the original nature of medicine. The main body is not only the medical staff, but also the patients and their families. This is very suitable to start with the intelligent medical treatment of hypertension, which has become a public problem. With the help of the intelligent medical treatment of digestive endoscopy, it is the main topic of general practice in the future to realize the intelligent medical treatment of more diseases.

Declaration of Competing Interest

The authors declare that they have no known competing financial interests or personal relationships that could have appeared to influence the work reported in this paper.

References

[1] V. Buch, G. Varughese, M. Maruthappu, Artificial intelligence in diabetes care, Diabet. Med. 35 (4) (2018) 56–61.
[2] Y.U. Bin, K. Kumbier, Artificial intelligence and statistics, Front. Inf. Technol. Electronic Eng. 19 (01) (2018) 6–9.
[3] F. Chiariotti, M. Condoluci, T. Mahmoodi, et al, SymbioCity: smart cities for smarter networks, Trans. Emerg. Telecommun. Technol. 29 (1) (2018) 23–25.
[4] O. Robert, P. Piotr, T. Agnieszka, Solving, "smart city" transport problems by designing carpooling gamification schemes with multi-agent systems: the case of the so-called "mordor of Warsaw", Sensors 18 (2) (2018) 141–142.
[5] S. Jha, E.J. Topol, Information and artificial intelligence, J. Am. College Radiol. 15 (3) (2018) 509–511.
[6] B. Majumdar, S.C. Sarode, G.S. Sarode, et al, Technology: artificial intelligence, Brit. Dental J. 224 (12) (2018) 916.
[7] T. Nawrocki, P.D. Maldjian, S.E. Slasky, et al, Artificial intelligence and radiology: have rumors of the radiologist's demise been greatly exaggerated?, Acad Radiol. 25 (8) (2018) 85–86.
[8] A.S. Cruz, H.C. Lins, R. Medeiros, et al, Artificial intelligence on the identification of risk groups for osteoporosis, a general review, Biomed. Eng. Online 17 (1) (2018) 12–14.

[9] K. Roman, Analysis and evaluation of the implementation level of the smart city concept in selected polish cities, Brain Broad Res. Artif. Intell. Neurosci. 9 (1) (2018) 138–145.
[10] E. Farrow, Organisational artificial intelligence future scenarios: futurists insights and implications for the organisational adaptation approach, leader and team, J. Futures Stud. 24 (3) (2020) 1–15.
[11] V.H. Buch, I. Ahmed, M. Maruthappu, Artificial intelligence in medicine: current trends and future possibilities, Br. J. Gen. Pract. 68 (668) (2018) 143–144.
[12] K. Guo, Y. Lu, G. Hui, et al, Artificial intelligence-based semantic internet of things in a user-centric smart city, Sensors 18 (5) (2018) 1341–1348.
[13] S. Khan, D. Paul, P. Momtahan, et al., Artificial intelligence framework for smart city microgrids: State of the art, challenges, and opportunities, in: Third International Conference on Fog & Mobile Edge Computing, IEEE, 2018, 7(4), pp. 283–288.
[14] L. Chen, P. Chen, Z. Lin, Artificial intelligence in education: a review, IEEE Access 8 (4) (2020) 75264–75278.
[15] A. Intelligence, A child's play, Technol. Forecast. Soc. Chang. 166 (3) (2021) 551–555.
[16] S. Zeadally, E. Adi, Z. Baig, et al, Harnessing artificial intelligence capabilities to improve cybersecurity, IEEE Access 8 (99) (2020) 23817–23837.
[17] C. Intahchomphoo, A. Vellino, O.E. Gundersen, et al, References to artificial intelligence in Canada's court cases, Legal Inf. Manage. 20 (1) (2020) 39–46.
[18] G. Mahadevaiah, R.V. Prasad, I. Bermejo, et al, Artificial intelligence-based clinical decision support in modern medical physics: selection, acceptance, commissioning, and quality assurance, Med. Phys. 47 (5) (2020) 96–97.
[19] T. Shiraishi, H. Murakami, Y. Iguchi, Diagnosis and treatment of cognitive impairment in Parkinson's disease, Brain Nerve = Shinkei kenkyū no shinpo 71 (8) (2019) 869–874.
[20] A.C. Pereiro, Guidelines for the diagnosis and treatment of Chagas disease, The Lancet 393 (10180) (2019) 1486–1487.
[21] J. Chen, Kenli, et al, A disease diagnosis and treatment recommendation system based on big data mining and cloud computing, Inf. Sci.: Int. J. 435 (4) (2018) 124–149.
[22] R. Veenhuizen, H. Nijsten, R.P. Van, et al, Huntington's disease outpatient clinic forfunctional diagnosis and treatment: coming to consensus: how long term care facility procedures complement specialist diagnosis and treatment, J. Huntingtons Dis. 7 (2) (2018) 189–192.
[23] H.J. Freeman, Role of biopsy in diagnosis and treatment of adult celiac disease, Gastroenterol. Hepatol. Bed Bench 11 (3) (2018) 191–196.
[24] L.I. Bin-Yin, X.U. Wei, Y.L. Deng, et al, Progress of translational research on the diagnosis and treatment of Alzheimer's disease and other dementias, Chinese J. Contemp. Neurol. Neurosurg. 18 (2) (2018) 95–98.
[25] M. Murata, Acute graft-versus-host disease: diagnosis and treatment, Japanese J. Clin. Hematol. 59 (5) (2018) 540–548.